



HAL
open science

Enhancement of humidity sensitivity of graphene through functionalization with polyethylenimine

Zeineb Ben Aziza, Kang Zhang, Dominique Baillargeat, Qing Zhang

► To cite this version:

Zeineb Ben Aziza, Kang Zhang, Dominique Baillargeat, Qing Zhang. Enhancement of humidity sensitivity of graphene through functionalization with polyethylenimine. *Applied Physics Letters*, 2015, 107 (13), pp.134102. 10.1063/1.4932124 . hal-01501915

HAL Id: hal-01501915

<https://unilim.hal.science/hal-01501915>

Submitted on 4 Apr 2017

HAL is a multi-disciplinary open access archive for the deposit and dissemination of scientific research documents, whether they are published or not. The documents may come from teaching and research institutions in France or abroad, or from public or private research centers.

L'archive ouverte pluridisciplinaire **HAL**, est destinée au dépôt et à la diffusion de documents scientifiques de niveau recherche, publiés ou non, émanant des établissements d'enseignement et de recherche français ou étrangers, des laboratoires publics ou privés.

Enhancement of humidity sensitivity of graphene through functionalization with polyethylenimine

Zeineb Ben Aziza, Kang Zhang, Dominique Baillargeat, and Qing Zhang

Citation: *Appl. Phys. Lett.* **107**, 134102 (2015); doi: 10.1063/1.4932124

View online: <http://dx.doi.org/10.1063/1.4932124>

View Table of Contents: <http://aip.scitation.org/toc/apl/107/13>

Published by the [American Institute of Physics](#)



Get the scoop on
science funding & policy

Free sign-up
for FYI emails

AIP American Institute of Physics

FYI is an authoritative news and resource center for federal science policy, with a focus on the physical sciences.

Enhancement of humidity sensitivity of graphene through functionalization with polyethylenimine

Zeineb Ben Aziza,^{1,2,3} Kang Zhang,² Dominique Baillargeat,^{1,3} and Qing Zhang^{1,2}

¹CINTRA CNRS/NTU/THALES, UMI 3288, Research Techno Plaza, 50 Nanyang Drive, Border X Block, Level 6, Singapore 637553

²School of Electrical and Electronics Engineering, Nanyang Technological University, Block S1, 50 Nanyang Avenue, Singapore 639798

³XLIM UMR 7252 Université de Limoges/CNRS, 123 Avenue Albert Thomas, 87060 Limoges, France

(Received 14 July 2015; accepted 16 September 2015; published online 30 September 2015)

In this work, we show that the sensing performance of graphene based humidity sensors can be largely improved through polymer functionalization. Chemical vapor deposited graphene is functionalized with amine rich polymer, leading to electron transfer from amine groups in the polymer to graphene. The functionalized graphene humidity sensor has demonstrated good sensitivity, recovery, and repeatability. Charge transfer between the functionalized graphene and water molecules and the sensing mechanism are studied systemically using field effect transistor geometry and scanning Kelvin probe microscopy. © 2015 AIP Publishing LLC.

[<http://dx.doi.org/10.1063/1.4932124>]

Humidity sensors are of great importance for industrial, environmental, and structural monitoring. Through monitoring and controlling humidity, corrosion, one of the most frequent causes of degradation of structures, can be prevented. Common humidity sensors essentially tell a change in the resistance,^{1,2} impedance,³ or even the mass of the sensing elements due to adsorbed water molecules.^{4,5} Graphene based gas sensors have been attracted a lot of attention mainly due to graphene 2D structure, which provides the largest sensing area per unit volume. The electrical properties of graphene are found to be very sensitive to the local perturbations on its surface due to surface charges and/or electronic density of states induced by adsorbed molecules.^{6–8}

However, the reported graphene based humidity sensors have several drawbacks. Massera *et al.* made use of exfoliated graphene and showed some promising results for humidity detection.⁹ As graphene is hydrophobic, this nature limits the sensing performance of pristine graphene based humidity sensors. In contrast, graphene derivatives, say, graphene oxide (GO) or reduced graphene oxide (RGO), have hydroxyl, carbonyl, and carboxyl functional groups on their basal planes so that the derivatives are hydrophilic and promising materials for humidity detection. Guo *et al.* used laser RGO films for humidity sensing.¹⁰ By tuning the laser power, the concentration of oxygen functional groups was controlled, resulting in a tunable response to humidity. Moreover, chemically RGO/polymer nanocomposite based humidity sensors have been reported to have a good sensitivity due to the hydrophilicity and multi-layer structure of polymer and RGO sensing films.¹¹

Nevertheless, these oxidation and reduction methods employed could cause covalent bonding, thereby destroying the sp^2 bonding of graphene lattice. These covalent approaches alter the transport properties of graphene and toxic oxidizing chemicals such as: sodium nitrate, potassium permanganate, and sulfuric acid were employed.¹² Efforts are still scaring to achieve a green and safe process for graphene oxidation.^{13,14}

In comparison with covalent bonding in GO and RGO, non-covalent methods could offer the π bonding on graphene basal plane and retain graphene unique electronic properties without necessarily making use of harsh chemicals. One of the approaches to non-covalently functionalize graphene was to coat graphene with a thin polymer layer. It was found by Dan *et al.*¹⁵ that Poly(methyl methacrylate) (PMMA) residues on graphene could largely enhance graphene sensitivity to water molecules by acting as an absorbent layer that concentrates molecules from the vapor within the polymer.

In this paper, we report on an efficient method to modulate the doping level of graphene and improve its sensitivity to humidity without causing damage to graphene. This method consists of graphene functionalization with polyethylenimine (PEI) that has been employed by other groups to induce electron doping to carbon nanotubes.^{16,17} PEI has also been used for polymer based humidity sensors, as PEI is known for its high hydrophilicity.^{18,19}

Monolayer chemical vapor deposited (CVD) graphene on copper foil was used in this work. Graphene was transferred on SiO_2 substrates by PMMA assisted transfer technique.²⁰ Branched PEI was used to functionalize graphene. It was adsorbed onto graphene by simple immersion in a 25 wt. % PEI/methanol solution for few hours. Thereafter, the sample was rinsed thoroughly with methanol and baked at 50 °C for 1 h.

The effectiveness of functionalization and the quality of graphene were first characterized using Raman spectroscopy (with exciting wavelength at 532 nm). Figure 1 shows the Raman spectra for functionalized and non-functionalized graphene. The G peak frequency is found to shift about 6 cm^{-1} downward and the 2D peak by 13 cm^{-1} upwards. These findings can be regarded as an indicator of doping, most likely electron doping in graphene.²¹ In addition, the intensity of the 2D peak and the ratio I_{2D}/I_G , considered as another indicators of doping,²² are also decreased for the functionalized graphene. The D band intensity slightly increased after introducing PEI molecules on graphene,

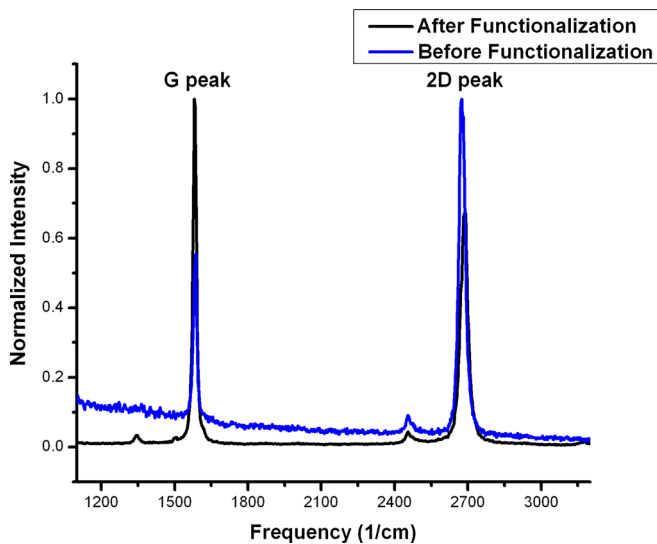


FIG. 1. Raman spectra of graphene before (blue) and after the (black) functionalization.

likely because these molecules increased the disorder of graphene basal plane.²³

In addition, electrical characterization was carried to determine the type of the doping. For this purpose, CVD single layer graphene based field effect transistors (GFET) were fabricated. GFETs were made on 285 nm silicon oxide/ p^+ -doped silicon substrate and had their graphene channel width of $4\ \mu\text{m}$. Figure 2 shows the optical image of these GFETs where the graphene ribbon with a size of $75\ \mu\text{m} \times 4\ \mu\text{m}$ appears as a darker strip located on the top of SiO_2 . Au/Ti (with thickness of 100 nm/10 nm) was patterned into the source and drain electrodes using optical lithography.

The GFETs' transfer characteristics under $V_{\text{ds}} = 20\ \text{mV}$ are shown in Figure 3. It is clearly seen that even after the functionalization, the performance of the GFETs was not much degraded and remained comparable to the performance before functionalization. In the case of non-functionalized graphene, the minimum channel conductance was observed at a positive threshold voltage (V_{th}), and this implies that the Fermi level was below the Dirac point and the graphene channel was hole doped. The hole doping can be explained by the presence of possible PMMA residues from the transfer

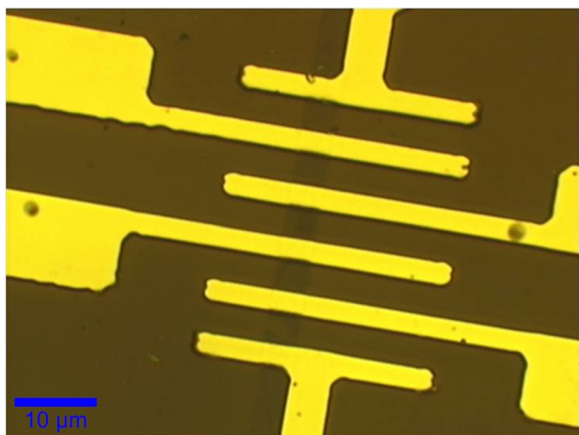


FIG. 2. Optical image of GFET fabricated on silicon oxide/ p^+ -doped silicon substrate; the channel width and length are both equal to $4\ \mu\text{m}$.

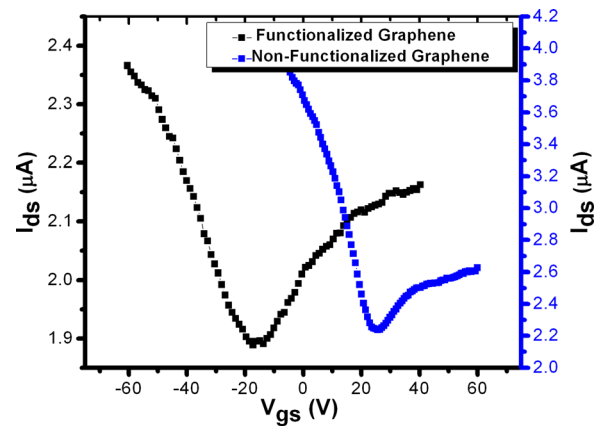


FIG. 3. The transfer curves under $V_{\text{ds}} = 20\ \text{mV}$ for GFETs with non-functionalized (blue) and functionalized (black) graphene.

process and adsorbates from environment.^{24,25} For the functionalized graphene, the V_{th} was shifted to a negative voltage, suggesting that PEI induced electron doping to graphene. This finding is similar to what was reported on PEI functionalized carbon nanotubes, where PEI was found to dope SWNTs with electrons.¹⁶ PEI induces electron transfer probably due to the high density amine groups. Doping by functional groups in irreversibly adsorbed polymer on graphene is found to be a simple approach of changing the doping level of graphene.

To characterize the functionalized graphene humidity sensing properties, a home built characterization system controlled by a Lab View program was used. Graphene based devices were placed in a gas chamber with dry nitrogen as the background gas. To measure humidity sensing characteristics of the graphene sample under different humidity levels, dry nitrogen was bubbled at various flow rates through a bubbler containing distilled water. The controlled humidity environments were achieved using mass flow controllers for monitoring the flow rate of dry nitrogen and bubbled nitrogen to obtain the desired relative humidity (RH). The RH values could be tuned from 10% to $>90\%$ by controlling the proportion of dry and humid nitrogen in the chamber. The tests were done at room temperature. Another set of FETs, made on 285 nm silicon oxide/ p^+ -doped silicon, with four interdigitated Au/Ti top electrodes with a 1 mm gap were fabricated to be adapted to the test cell. The applied voltage between the top electrodes was 100 mV. The change in the resistance of graphene between the electrodes upon exposure to various relative humidities was monitored as the sensing signal. The resistance was found to decrease with increasing humidity. The sensitivity was determined by the percentile resistance change or, in other words, by the ratio $R/R_0 \times 100$, where R_0 is the initial resistance of the sensors in dry environment and R is the resistance corresponding to the different exposures to various RH levels.

From Figure 4, one can notice that both sensors show resistance decrease with increasing RH. The functionalized sensor responded more apparently to humidity, about 10 times more than non-functionalized graphene. The sensitivity of the functionalized graphene was further tested under different humidity levels and longer time intervals. In Figure 5, one can find that the functionalized graphene sensor

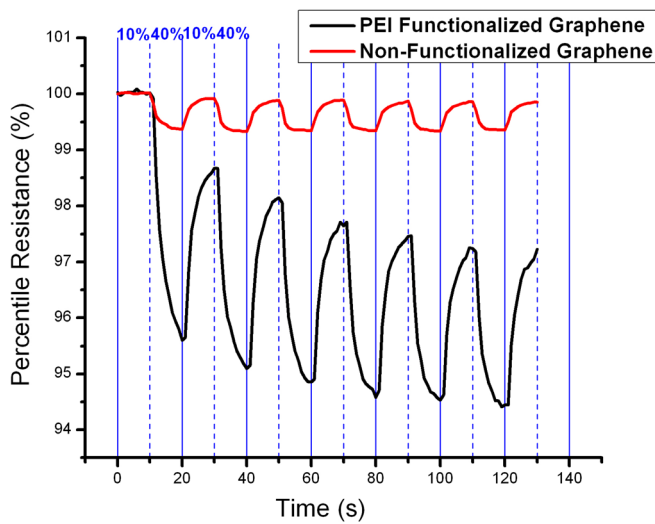


FIG. 4. Humidity responses (RH: 10% \rightarrow 40%) at room temperature for non-functionalized (red) and functionalized (black) graphene.

exhibited a very good reproducibility thanks to its sensitivity to water molecules and the fast recovery. This response was better than the reported performance of bilayer CVD graphene that exhibited about 3% resistance change for a variation of RH from 44% to 55% (Ref. 26) and chemically exfoliated graphene that showed unstable response with varying the humidity levels.⁹ All these suggest that PEI functionalized graphene is a promising material for humidity sensing applications.

According to the density functional theory, water molecules can act as acceptors or donors after they adsorb onto pristine graphene surface, depending on the relative position of their highest occupied molecular orbital and lowest occupied molecular orbital with respect to the graphene Dirac point.²⁷ Indeed, Leenaerts *et al.* discussed different interactions between water molecule orbitals and graphene and they found out that one of the possible orientations, where a water molecule acted as an acceptor on graphene, could be energetically selected on perfect graphene. Thus, the acceptor character is energetically favored with an electron transfer from

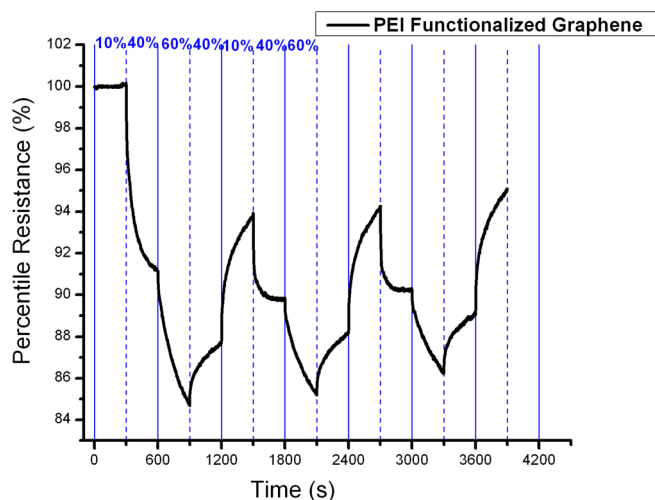


FIG. 5. Response at room temperature of functionalized graphene to various humidity level cycles (10% \rightarrow 40% \rightarrow 60% \rightarrow 40% \rightarrow 10%).

graphene to the adsorbed water molecule of about 0.025 e.²⁷⁻²⁹ This acceptor behavior of H₂O is also consistent with the previous experimental results.^{6,30}

Before functionalization, the resistance of the graphene sensors decreased when exposed to a high level of humidity. This is consistent with the explanation that adsorbed water molecules induce hole doping in the graphene. As mentioned above, before functionalization, graphene showed p type with its Fermi level below the Dirac point. Once water molecules adsorb on the graphene surface and cause hole doping, the Fermi level would shift further away the Dirac point, the resistance of the graphene would decrease.

As discussed above, the functionalized graphene showed n-doped. The resistance of the functionalized graphene was sharply decreased under high humidity levels, suggesting that water molecules act likely as donors in this case.

To better understand the sensing mechanism governing the water molecules adsorption onto PEI-functionalized graphene, scanning Kelvin probe microscopy (SKPM) measurements and electrical characterization of the tested graphene devices were performed.

SKPM experiments on single and few layer graphene have been already reported.^{31,32} It has been shown that the work function of graphene can be tuned by changing the carrier density.³¹

In this experiment, the work function difference between the functionalized graphene and gold electrode was characterized by SKPM scanning at low and high humidity levels. A conductive tip coated with Pt/Ir with a resonant frequency of 75 kHz and a force constant of 2.8 N/m was used in this work. To control the humidity, two dry N₂ gas lines with one line passing through a bubbler containing DI water were introduced in an atomic force microscopy (AFM) chamber. The desired humidity values were reached by varying the flow rates of wet/dry nitrogen. A Testo hygrometer was used to measure the RH levels in the AFM chamber with an error of less than 3%.

SKPM images the contact potential difference (Δ CPD) between the probe and the materials under scan. The value of an SKPM image, i.e., the Δ CPD, represents the voltages applied to the probe so that there is no electrostatic force between the probe and the material under scan. According to the Kelvin Probe principle,³³ the SKPM image value can be calculated by the work function difference between the probe and the materials and a higher SKPM value represents a lower work function of the sample. As shown in Figures 6(a) and 6(b), the SKPM image of gold electrode is always brighter than the functionalized graphene, suggesting a lower work function of the gold than graphene, i.e., a higher electron Fermi level of gold than graphene before they are brought into contact. Therefore, a net electron transfer from gold to graphene occurs as they are brought into contact. As shown in Figure 6(c), when RH is increased from \sim 20% to \sim 50%, the Δ CPD of graphene is increased by \sim 30 mV. Given the surface potential of gold remains almost unchanged for higher humidity, being consistent with the results reported on water adsorption behavior on the surface of gold,³⁴ the increase of Δ CPD in graphene represents a lowering of the graphene work function, suggesting that the electron Fermi level of graphene becomes higher at higher RH. Clearly,

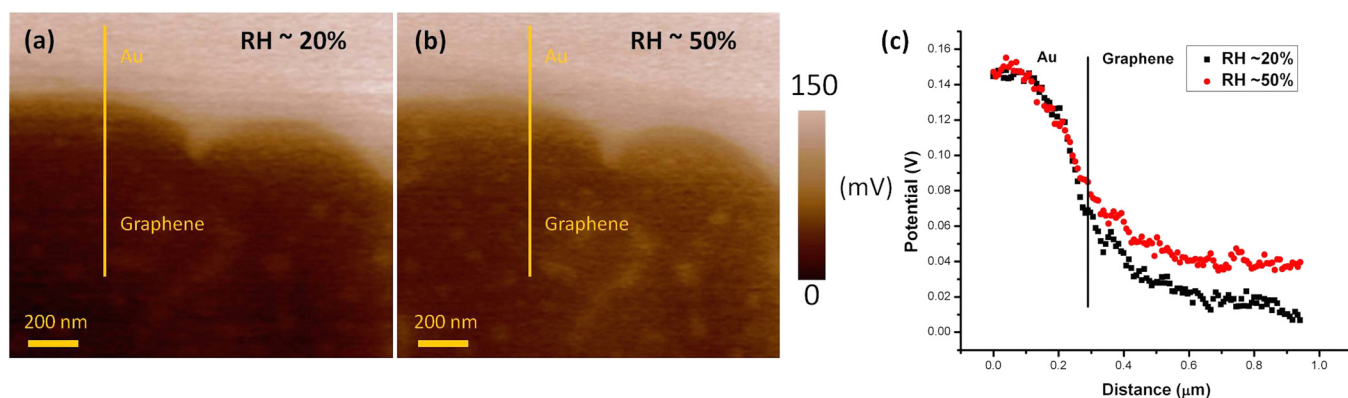


FIG. 6. SKPM images of functionalized graphene at different humidity levels: (a) RH \sim 20%; (b) RH \sim 50%. (c) The graph shows the potential variations corresponding to the same selected location marked with the yellow line in (a) and (b) for RH \sim 20% (black) and RH \sim 50% (red).

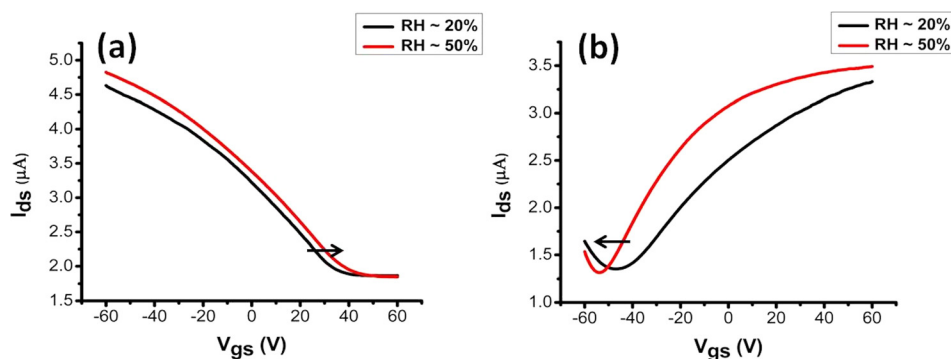


FIG. 7. Transfer curves under $V_{ds} = 10$ mV for (a) non-functionalized and (b) PEI-functionalized graphene at different humidity levels: RH \sim 20% (black) and RH \sim 50% (red).

water molecules cause electron doping to the functionalized graphene. These SKPM results are consistent with the previous findings from the resistance variations under different humidity levels.

To confirm these results, the transfer characteristics of the FET samples were also measured at RH \sim 20% and RH \sim 50% as shown in Figures 7(a) and 7(b). We found out that for non-functionalized graphene V_{th} is slightly shifted to a more positive value for higher humidity due to the hole doping from water molecules. However, for PEI functionalized graphene, V_{th} was further shifted to a more negative voltage, suggesting that water molecules induce electron doping to functionalized graphene. These measurements are in agreement with the above SKPM results, suggesting that water molecules show acceptor behavior on non-functionalized graphene, whereas they exhibit a donor behavior on PEI-functionalized graphene.

In summary, we showed experimentally the influence of PEI functionalization of graphene on humidity detection of the graphene based humidity sensors. Upon the functionalization, the graphene is apparently doped with electrons, probably caused by the high density amine groups in PEI. The functionalized graphene based sensors exhibit clearly a higher sensitivity and repeatability towards water molecules. Absorbed water molecules may act as electron donors on the functionalized graphene, while they may withdraw electrons on non-functionalized graphene.

¹S. Si, S. Li, Z. Ming, and L. Jin, *Chem. Phys. Lett.* **493**(4), 288–291 (2010).

²Y. Zhang, K. Yu, D. Jiang, Z. Zhu, H. Geng, and L. Luo, *Appl. Surf. Sci.* **242**(1), 212–217 (2005).

³H. Bi, K. Yin, X. Xie, J. Ji, S. Wan, L. Sun, M. Terrones, and M. S. Dresselhaus, *Sci. Rep.* **3**, 2714 (2013).

⁴A. Erol, S. Okur, B. Comba, O. Mermer, and M. C. Arikan, *Sens. Actuators B* **145**(1), 174–180 (2010).

⁵P. G. Su and Y. P. Chang, *Sens. Actuators B* **129**(2), 915–920 (2008).

⁶F. Schedin, A. K. Geim, S. V. Morozov, E. W. Hill, P. Blake, M. I. Katsnelson, and K. S. Novoselov, *Nat. Mater.* **6**, 652 (2007).

⁷O. Leenaerts, B. Partoens, and F. M. Peeters, *Microelectron. J.* **40**, 860 (2009).

⁸L. Kong, A. Enders, T. S. Rahman, and P. A. Dowben, *Condens. Matter* **26**, 443001 (2014).

⁹E. Massera, V. La Ferrara, M. Miglietta, T. Polichetti, I. Nasti, and G. Di Francia, *Chem. Today* **29**(1) (2011).

¹⁰L. Guo, H. B. Jiang, R.-Q. Shao, Y. L. Zhang, S.-Y. Xie, J. N. Wang, X. B. Li, F. Jiang, Q. D. Chen, T. Zhang, and H. B. Sun, *Carbon* **50**(4), 1667–1673 (2012).

¹¹D. Zhang, J. Tong, and B. Xia, *Sens. Actuators B* **197**, 66–72 (2014).

¹²W. S. Hummers and R. E. Offeman, *J. Am. Chem. Soc.* **80**, 1339 (1958).

¹³D. C. Marcano, D. V. Kosynkin, A. Sinitskii, Z. Sun, A. Slesarev, L. B. Alemany, W. Lu, and J. M. Tour, *ACS Nano* **4**, 4806 (2010).

¹⁴J. Chen, B. Yao, C. Li, and G. Shi, *Carbon* **64**, 225 (2013).

¹⁵Y. Dan, Y. Lu, N. J. Kybert, Z. Luo, and A. T. C. Johnson, *Nano Lett.* **9**(4), 1472–1475 (2009).

¹⁶M. Shim, A. Javey, N. Wong Shi Kam, and H. Dai, *J. Am. Chem. Soc.* **123**, 11512–11513 (2001).

¹⁷P. Qi, O. Vermesh, M. Grecu, A. Javey, Q. Wang, and H. Dai, *Nano Lett.* **3**(3), 347–351 (2003).

¹⁸B. Chachulski, J. Gebicki, G. Jasinski, P. Jasinski, and A. Nowakowski, *Meas. Sci. Technol.* **17**, 12–16 (2006).

¹⁹T. Zajt, G. Jasinski, and B. Chachulski, *Proc. SPIE* **5124**, 130–137 (2003).

²⁰Z. B. Aziza, Q. Zhang, and D. Baillargeat, *Appl. Phys. Lett.* **105**, 254102 (2014).

²¹A. Das, S. Pisana, B. Chakraborty, S. Piscanec, S. K. Saha, U. V. Waghmare, K. S. Novoselov, H. R. Krishnamurthy, A. K. Geim, A. C. Ferrari, and A. K. Sood, *Nat. Nanotechnol.* **3**, 210 (2008).

²²Z. H. Ni, T. Yu, Z. Q. Luo, Y. Y. Wang, L. Liu, C. P. Wong, J. Miao, W. Huang, and Z. X. Shen, *ACS Nano* **3**, 569 (2009).

²³X. Dong, D. Fu, W. Fang, Y. Shi, P. Chen, and L. J. Li, *Small* **5**(12), 1422–1426 (2009).

- ²⁴A. Pirkle, J. Chan, A. Venugopal, D. Hinojos, C. W. Magnuson, S. McDonnell, L. Colombo, E. M. Vogel, R. S. Ruoff, and R. M. Wallace, *Appl. Phys. Lett.* **99**, 122108 (2011).
- ²⁵H. E. Romero, N. Shen, P. Joshi, H. R. Gutierrez, S. A. Tadigadapa, J. O. Sofo, and P. C. Eklund, *ACS Nano* **2**(10), 2037–2044 (2008).
- ²⁶M. C. Chen, C. L. Hsu, and T. J. Hsueh, *IEEE Electron Device Lett.* **35**(5), 590–592 (2014).
- ²⁷O. Leenaerts, B. Partoens, and F. M. Peeters, *Phys. Rev. B* **77**, 125416 (2008).
- ²⁸X. Lin, J. Ni, and C. Fang, *J. Appl. Phys.* **113**, 034306 (2013).
- ²⁹T. O. Wehling, M. I. Katsnelson, and A. I. Lichtenstein, *Chem. Phys. Lett.* **476**, 125 (2009).
- ³⁰Q. Huang, D. Zeng, S. Tian, and C. Xie, *Mater. Lett.* **83**, 76–79 (2012).
- ³¹Y. J. Yu, Y. Zhao, S. Ryu, L. E. Brus, K. Kim, and P. Kim, *Nano Lett.* **9**, 3430 (2009).
- ³²D. Ziegler, P. Gava, J. Güttinger, F. Molitor, L. Wirtz, M. Lazzeri, A. M. Saitta, A. Stemmer, F. Mauri, and C. Stampfer, *Phys. Rev. B* **83**, 235434 (2011).
- ³³I. D. Baikie, U. Petermann, A. Speakman, B. Lägel, K. M. Dirscherl, and P. J. Estrup, *J. Appl. Phys.* **88**, 4371 (2000).
- ³⁴L. Q. Guo, X. M. Zhao, Y. Bai, and L. J. Qiao, *Appl. Surf. Sci.* **258**, 9087–9091 (2012).